I&EC research
Industrial & Engineering Chemistry Research

pubs.acs.org/IECR

Article

Production of Dimethyl Carbonate Using a Zirconium−Praseodymium-Based Catalyst from Methanol and Propylene Carbonate: An Experimental and DFT Study

Surbhi Dahiya, Pankaj Kumar, Vimal Chandra Srivastava,* and Vimal Kumar

Cite This: *Ind. Eng. Chem. Res.* 2023, 62, 6920−6931

Read Online

ACCESS | Metrics & More | Article Recommendations | Supporting Information

ABSTRACT: In the presence of specific catalysts made using the coprecipitation approach, methanol and propylene carbonate (PC) react to yield dimethyl carbonate (DMC) as well as propylene glycol (PG) through the transesterification process. The catalytic activity of mixed zirconium and praseodymium oxides ($Zr_{1-x}Pr_xO_2$, x = 0.01−0.05), synthesized by coprecipitation, was investigated in this work towards the formation of DMC and PG. The process involves the transesterification of methanol and propylene carbonate to occur in a batch reactor. Numerous methods, including X-ray diffraction (XRD), scanning electron microscopy (SEM), Fourier transform infrared (FTIR) spectroscopy, and CO_2-TPD have been used to characterize the catalysts. The goal of the study is to ascertain how the combination of praseodymium and zirconium affects the yield and selectivity of DMC. DFT calculations have been performed for the catalytic system. Becke's hybrid three-parameter nonlocal exchange functional (B3), the Lee−Yang−Parr (LYP) correlation functional (B3LYP), and the SDD basis set were all used to optimize the geometries. $Zr_{0.96}Pr_{0.04}O_2$ was found to have the best PC conversion (95.9%), while its yield and selectivity were 52.5% and 54.7%, respectively, at 165 °C, methanol/PC ratio = 6.5, and time of 3 h.

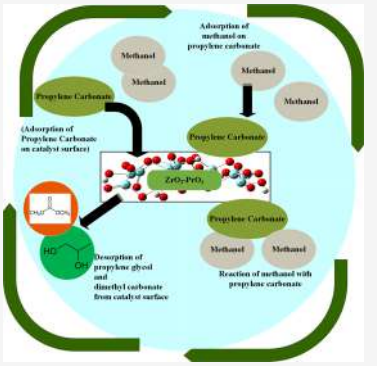

1. INTRODUCTION

The concept of sustainable development of processes in the manufacture and use of chemicals so that they become ecologically benign is what the term "green chemistry" refers to.[1] This necessitates the employment of chemicals that can replace poisonous, dangerous, nonbiodegradable materials that have caused pollution of the air, water, and other aspects of the ecosystem.[2] Dimethyl carbonate, an organic carbonate formed during the research for this publication, has a high oxygen content (53%) and is a very good substitute for the fuel and paint industries.[3]

Due to its versatility and environmental friendliness, dimethyl carbonate is in demand across a range of industries, from polymer to pharmaceuticals, where it can be employed as a detergent, surfactant, etc.[4] It has replaced itself as a raw material for the manufacturing of numerous compounds, such as diphenyl carbonate and glycerol carbonate, and it is an effective replacement for toxic gases like phosgene.[5] It can be used to produce a variety of things, including polymers, insecticides, flavorings, meals, solvents, and more. It has a high octane rating, which enhances the antiknocking capabilities of fuels.[6] It has low Reid vapor pressure (RVP) and reduced nitrogen and sulfur oxide emissions, therefore, is used as a fuel additive. Its various properties include a melting point of 4.6 °C, a boiling point of 90.3 °C, an ignition temperature of 458 °C, a cetane number of 45, and a specific gravity of 1.07.[7]

It is a secure substitute that can be utilized as a solvent in the paint and polymer industries, as well as an additive in gasoline.[8] It can be made through a number of processes, including a direct synthesis route that utilizes CO_2 and methanol to produce DMC, transesterification, urea alcoholysis, methanolysis of phosgene, etc.[9] Utilizing the surplus carbon dioxide from the fuel and other industries is made easier by the direct synthesis method from carbon dioxide. Its synthesis by carbon dioxide is not only environmentally friendly but also aids in the replacement of traditional processes that use toxic chemicals like phosgene.[10] However, there is a thermodynamic limit to how much DMC can be produced from carbon dioxide. Due to the great stability of the CO_2 molecule in nature and the creation of water during the reaction, which results in very low conversion and selectivity, the reaction is not very feasible.[11]

Therefore, it becomes important to adopt the other route, transesterification, which gives higher yield and selectivity in comparison to the direct synthesis route. This route has

Received: January 21, 2023
Revised: April 3, 2023
Accepted: April 7, 2023
Published: May 1, 2023

https://doi.org/10.1021/acs.iecr.3c00168
Ind. Eng. Chem. Res. 2023, 62, 6920−6931

Scheme 1. Transesterification Reaction of Propylene Carbonate with Methanol[24]

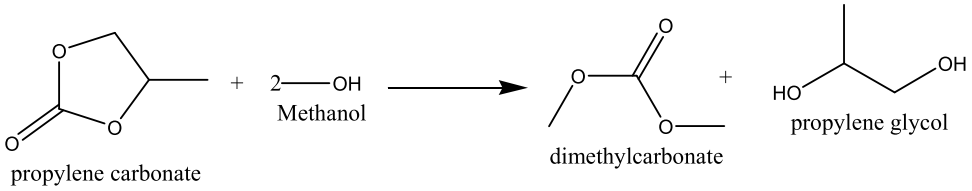

various added advantages as it does not corrode the equipment and does not produce waste.[12]

Several catalysts are used that can help in overcoming the activation energy of the reaction, thus enabling this reaction to occur in the favor of the product. The heterogeneous catalysts such as bimetallic catalysts gave better results in terms of yield as well as selectivity due to the active basic and acidic sites available for the adsorption of reactants.[13] Researchers have used several catalysts such as ZrO_2, CeO_2, MgO−CeO_2, ZnO, Fe−Zn, and ion-exchange resins and found that these catalysts were effective for this reaction.[14,15] Kumar et al.[16] used ceria−zinc catalysts impregnated over alumina, titania, and silica and achieved a DMC yield of 77%. Liao et al.[17] utilized solid-based catalysts derived from Ca−Al−X (X = F^-, Cl^- and Br^-) and achieved a PC conversion of 68.8%. Kumar et al.[18] used N_2-functionalized graphene oxide nanosheets, an innovative approach toward carbon-based catalysts, and achieved a DMC yield of 50%.

There have been several attempts to combine rare-earth metals or transition metals in order to bring better performance in reaction conditions. Pr is one such element, from the family of rare-earth metals, where it is combined in a certain ratio with other metals and helps increase the yield and selectivity of the product in several chemical reactions. It has been studied that lanthanides possess certain properties such as diverse electronic band structures and a dynamic coordinated approach that provide them excellent optical properties and enhanced photocatalytic activity in many ways.[19] In other work, it has been demonstrated that the effect of Pr has influenced the oxygen defects/mobility in CeO_2-based materials and altered certain basic and acidic properties.[20] It has been shown that doping with Pr^{3+} may induce oxygen vacancies in the Prins condensation−hydrolysis cycle by charge compensation, causing the lattice to distort and allowing the production of complexes, namely of type Pr_3O_8.[21] For the VOCs' catalytic combustion, incorporation of elements such as Pr helps in reducing the metal oxides such as Pr and Ce metallic oxides, creating oxygen vacancies and releasing the capability of metallic oxides.[22]

Though the available literature has reported several catalysts to be utilized in the transesterification reaction, however, the synthesis of Zr−Pr-based catalyst in this work has its own advantages. Using this catalyst does not leave any residue during the reaction. The amount of Pr in the catalyst is present in a smaller amount as compared to the other dopants such as Zr, Ce, Fe, Cu, etc. used in several catalysts, which makes the catalyst cost-effective. The yield and selectivity obtained are significant if compared to the amount of the catalyst taken. Pr, being the rare-earth metal, has the capability of forming complexes with alcohols such as methanol, which leads to the better adsorption of raw materials such as methanol and propylene carbonate on its surface, thereby yielding DMC in good amounts. The mixing of Pr in the catalyst increases the basicity, which is a very effective factor for the transesterification reaction. Several catalysts that employ CaO give better yield but poor stability.[17] The catalyst Au/CeO_2 has been reported for its use in this reaction but the yield obtained was low. Similarly, the ZnO catalyst gave a low yield toward DMC production.[23] Hence, future work could focus on doping or mixing Pr with several metals or even organic compounds including polymers to produce catalysts that may promote the reactions toward the product side.

The transesterification reaction of methanol and PC can be enumerated as Scheme 1.

The focus of this work in its present form is the production of DMC and PG through the development of mixed oxide catalysts of zirconium and praseodymium in various ratios. Praseodymium, being the rare-earth metal, has an added advantage of f-orbitals that helps in the transition of states toward oxidation, enabling the suitability of the transesterification reaction. The prepared catalysts were studied extensively using certain techniques such as X-ray diffraction (XRD), N_2 sorption, FTIR, XPS, and FESEM. Further, the study is made to determine the modification of properties (basicity) in these catalysts using CO_2-TPD. The batch reactor was used to study the transesterification, or a further reaction, of methanol and propylene carbonate that produces DMC and PG. In addition to the reaction, the material is centrifuged to regenerate the catalysts after the reaction, and the efficiency of this process is evaluated during the production process.

2. EXPERIMENTAL SECTION

2.1. Catalyst Synthesis. *2.1.1. Synthesis of Zr−Pr Metal Oxides with Various Molar Ratios.* Coprecipitation was used to create a variety of zirconia−praseodymium ($Zr_{1-x}Pr_xO_2$, x = 0.01−0.05) catalysts. Using zirconium(IV) oxynitrate hydrate and praseodymium nitrate hexahydrate, coprecipitation was used to create ZrO_2/PrO_2 catalysts with various targeted molar ratios (Pr/Zr = 0.01, 0.02, 0.03, 0.04, 0.05). Separately dissolved in about 50 mL of demineralized water, the two precursors were then combined with constant stirring to achieve the appropriate molar Zr/Pr ratios of 0.01, 0.02, 0.03, 0.04, and 0.05. Furthermore, 50 mL of demineralized water was used to prepare a 1M NaOH solution. To precipitate out the mixed oxides, this NaOH solution has been added to the above-prepared solution (precursor). This solution was aged for around 12 h under vigorous stirring with 450 rpm and then washed with demineralized water for the pH adjustment to 7. This catalyst was dried in an oven at a temperature of 80 °C. The materials were calcined at 700 °C (as per the TGA results) under airflow for 4 h. The synthesized catalysts were denoted as $Zr_{0.99}Pr_{0.01}O_2$ (ZrPr(1)), $Zr_{0.98}Pr_{0.02}O_2$ (ZrPr()), $Zr_{0.97}Pr_{0.03}O_2$ (ZrPr(3)), $Zr_{0.96}Pr_{0.04}O_2$ (ZrPr(4)), and $Zr_{0.95}Pr_{0.05}O_2$ (ZrPr(5)) for catalysts having Zr/Pr molar ratios of 0.01, 0.02, 0.03, 0.04, and 0.05, respectively.

2.2. Physical Characterization. To study the thermogravimetric analysis, a thermal analyzer was used. For this, the sample of the catalyst was put down in an alumina crucible and

https://doi.org/10.1021/acs.iecr.3c00168
Ind. Eng. Chem. Res. 2023, 62, 6920−6931

then heated between 30 and 1000 °C at a 10 °C/min rate under the flow of oxygen (40 cm^3/min).

With the help of a Bruker ARS D8 advanced powder X-ray diffractometer and Cu Ka (0.154 nm) as an X-ray source, XRD patterns of ZrPr catalysts were captured. The wide-angle range of 5−90° and 40 kV were scanned at a pace of 2°/min. Additionally, the Debye−Scherer equation ($D = 0.9\ \lambda/b \cos\theta$) was utilized for calculating the crystalline size of the catalysts. Further, Bragg's equation or $n\lambda = 2d \sin\theta$ was employed in calculating the interlayer spacing. The catalysts were studied further for the morphological characterization using FESEM (Carl-Zeiss-Gemini) operated at 10 kV. The functional groups were determined and analyzed using XPS (PHI 5000 versa probe III).

The study for the textural properties was done using the catalysts that were characterized using a multipoint N_2-adsorption−desorption setup equipped at −195 °C using a Micromeritcs ASAP 2020 apparatus. First, the catalysts were degassed at 200 °C under the N_2 gas flow to ensure that no adsorbed impurities remained on the surface of the catalysts. Once the degassing happened, the surface area and the pore volume diameter were calculated as the surface properties. These were estimated using the Brunauer−Emmett−Teller (BET) and Barrett−Joyner−Halenda (BJH) models, respectively. For studying these models, the isotherm's desorption facilitated calculating the pore diameter and pore size distribution via the BJH equation.

A Micromeritics Chemisorb 2720 fitted with a thermal conductivity detector (TPD) helped in determining the basic properties or basicity precisely of the catalysts through CO_2-TPD. In the determination of basicity, several steps are followed. First, the catalyst sample is put in a quartz U-tube, which is then allowed to activate at 200 °C under the flow of He gas (20 cc/min) for nearly 6 h. Once this is done, then this same sample is allowed to be cooled to 50 °C, which is further allowed for CO_2 adsorption by maintaining the 10% CO_2/He flow of 20 cc/min in order to find the basicity. Then, the desorption profile is further recorded in the range of 50−900 °C by maintaining the heating rate at 10 °C/min under He flows (20 cc/min). After this process, CO_2-TPD gets studied at TCD.

An FTIR spectrophotometer (Thermo Nicolet, Model Magna 760) helped in studying the FTIR spectra of the catalysts. The powered catalysts were converted into KBr pellets and scanned in the 400−4000 cm^{-1} range. Once the reaction occurred in the batch reactor, the product was analyzed using the GC equipped with a flame ionization detector (FID) and an HP-5 (30 m 0.25 mm, 0.25 m) capillary column and an HP-5 (30 m 0.25 mm, 0.25 m) capillary column.

2.3. Catalyst Performance. The catalyst performance was determined using a set of catalysts (ZrPr) and placing them in a high-pressure autoclave batch reactor of 100 mL. Along with the catalysts, the raw materials methanol and propylene carbonate were also placed simultaneously in the reactor along with the stirring bead for proper mixing. The reaction involves the transesterification of PC and methanol. The reactants are put in a certain molar ratio (methanol/PC = 3−8) and catalyst (3−8 wt % of PC). The products produced are DMC and PG. During the reaction, the temperature is maintained between 150 and 170 °C, and the analysis of the end products is done through gas chromatography (GC). At the beginning of the reaction, nitrogen is purged in the reactor in the range of 5−15 bar and then the autogenic pressure of about 20 bar is maintained. The analysis of DMC yield, PC conversion, DMC selectivity as well as TOF (turn over frequency) is calculated after the data is obtained from GC.

3. RESULTS AND DISCUSSION

3.1. Catalyst Characterization. The thermogravimetric analysis (TGA) is represented in Figure 1a. It is carried out to determine the weight loss that occurs as a function of T (temperature).[18] During the study, it was found that the degradation occurs in steps described in the manner that at a temperature near 100 °C, there is a removal of water molecules attached to the catalyst surface, meaning that there is a removal of surface-bound (adsorbed) H_2O molecules. Between 200 and 600 °C, there may occur loss of labile functional groups along with intercalated H_2O molecules that may have a presence in the catalyst interlayers. After 600 °C, there may occur pyrolysis, and oxygen-containing functional groups such as volatiles may convert to CO or CO_2 after which the catalyst reaches the stable structure, which becomes effective enough for calcination in an air furnace.[18]

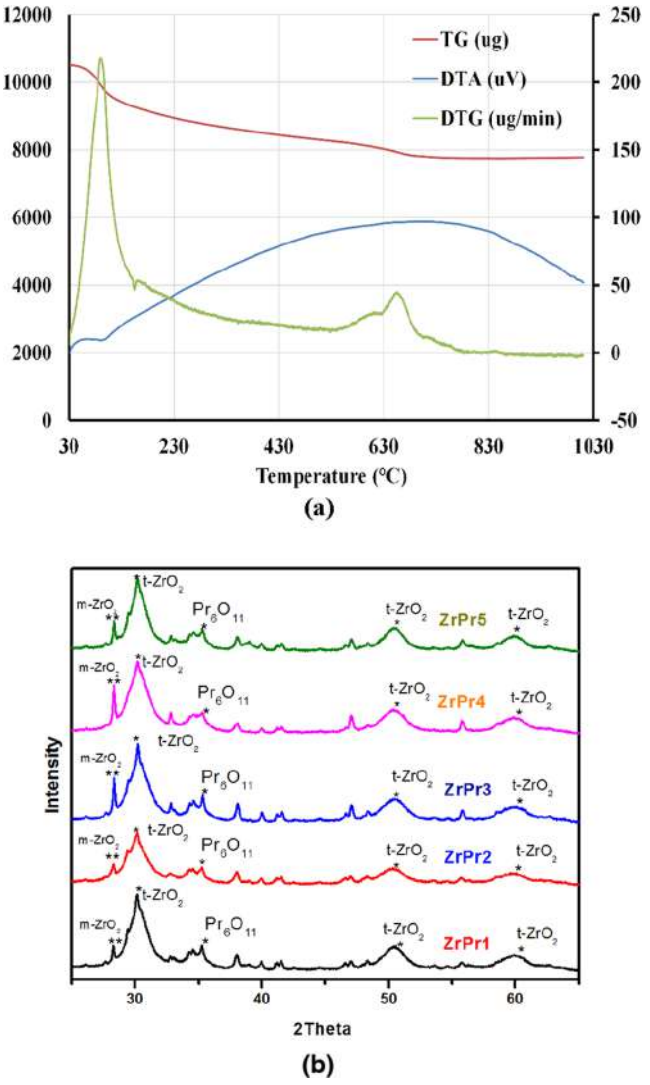

Figure 1. (a) TGA of the ZrPr(4) catalyst and (b) XRD of ZrPr(1), ZrPr(2), ZrPr(3), ZrPr(4), and ZrPr(5).

https://doi.org/10.1021/acs.iecr.3c00168
Ind. Eng. Chem. Res. 2023, 62, 6920−6931

The XRD pattern of the mixed oxides is shown in Figure 1b. It shows that there occurs a peak in the catalysts ZrPr(5), ZrPr(4), and ZrPr(3) at around $2\theta = 28.5°$, which corresponds to the phase transition of ZrO_2 from a monoclinic to tetragonal phase.[24] This kind of transition gives a metastable structure that enables a better reaction (in this case) as it provides a stable structure for the reactants to adsorb on the catalyst sites. For less concentration of Pr, this type of transition did happen in a smaller manner. It may be ascribed to the reason that Pr in higher concentration enabled this transition by interfering with ZrO_2 in a superficial manner. The diffraction at around 30.2, 34.6, and 50° corresponds to ZrO_2, corresponding to the monoclinic and tetragonal phases, which are found in all of the prepared catalysts. The characteristic peaks corresponding to 2θ = 30.2, 34.5, 50.2, and 60.2° are in accordance with the planes (1 0 1), (1 1 0), (2 0 0), and (2 1 1) of the tetragonal phase of zirconia. In the case of ZrPr(1) and ZrPr(2), the structure remains intact even when the very low-intensity peak of PrO_2 is found. The crystalline size is calculated using the Debye−Scherer equation (Table 1). The average crystalline

Table 1. Crystalline and Surface Properties of the Catalysts

	plane (1 0 1)				
sample	2θ (°)	d (nm)	crystalline size (nm)	BET surface area (m^2/g)	pore volume (cm^3/g)
ZrPr(1)	30.14	0.296	43.5	9	0.01
ZrPr(2)	30.16	0.296	43.5	12	0.01
ZrPr(3)	30.20	0.295	63.3	23	0.02
ZrPr(4)	30.17	0.295	43.5	39	0.03
ZrPr(5)	30.16	0.295	43.5	23	0.02

size for ZrO_2 is 43.8 nm, whereas the size is smaller for all of the catalysts except ZrPr(3). This abrupt size increase in ZrPr(3) may have occurred, which may be due to the fact that the larger size of the Pr^{3+} ion would not have fitted in the lattice structure due to the transition of the oxidation state of Pr toward Pr^{3+}.[25] The d-spacing, which is calculated using the Braggs equation, gives the value at around 0.295 nm, corresponding to the peak of 30.20° for all of the catalysts, which means that there occurs not much differentiation in terms of functional groups such as that of volatiles that may be attached to the catalysts and reflects that Zr is predominantly mixed with Pr.[26]

The FTIR spectrum of the prepared catalysts before the reaction and after the reaction is studied (Figure 2). The stretching near the wavenumber 3600−3200 cm^{-1} is due to the hydroxyl group present in the interlayers of the catalyst.[27] Further, the peaks observed near 1480−1500 cm^{-1} are related to the C−N bond that may be present in the interlayers due to incomplete degradation during the preparation. The peak near 2360 cm^{-1} in ZrPr(3) indicates Zr−OH (zirconium hydroxyl bond) and near 500 cm^{-1} indicates the stretching vibration of Zr−O of the ZrO_2 phase. In some catalysts, the peaks are present near 1614 cm^{-1}, which belong to the C═O bond vibration, and the peaks near 720 cm^{-1} show that the Zr−O−Zr bonds are formed in the catalysts.

The FTIR spectra of the ZrPr(4) catalyst have been studied after the reaction has occurred (Figure 2). This gives the enhanced details of the species that gets adsorbed onto the surface of the catalyst because of the transesterification reaction. There is also a noticeable fact that the peaks in the certain region became sharper, indicating the enhanced bond

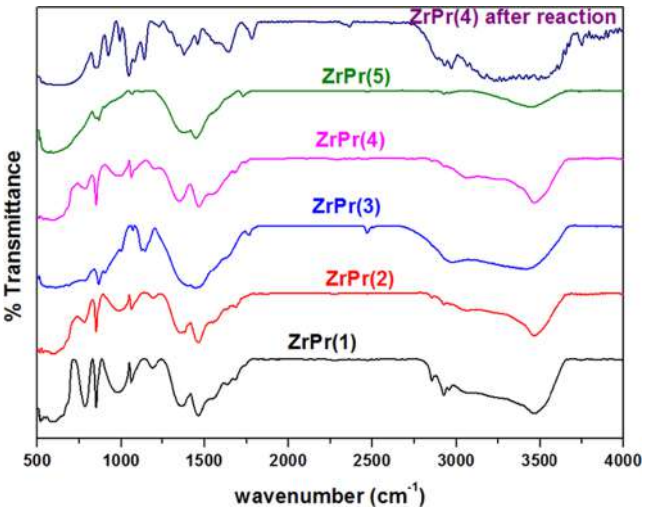

Figure 2. FTIR of ZrPr(1), ZrPr(2), ZrPr(3), ZrPr(4), and ZrPr(5) before the reaction and ZrPr(4) after the reaction.

formation in the different ranges of spectra. The bond that was not initially present in ZrPr(4) at around 2360 cm^{-1} indicates that the presence of a zirconium hydroxyl bond became visible after the reaction. The peaks near the region 1465 and 1392 cm^{-1} are mainly ascribed to the formation of polydentate carbonates. As per the literature, the peaks centered at around 1600 and 1570 cm^{-1} are mainly the peaks of hydrogen carbonates (HCs) and bidentate carbonates (BCs). This provides a mechanistic study that carbonates (DMCs) are formed during the reaction. The surface of the catalyst gives an amenable environment for the formation of Zr−OCH_3 as methanol comes near its surface.

The nitrogen adsorption−desorption isotherm is shown in Figure S1a. There is an observation of a type 1V isotherm with a type H3 hysteresis loop in the high range of relative pressure. This is an indication of the slit-arranged mesoporous structure of the catalysts. The adsorption amounts are different than the desorption mounts; it results in the hysteresis loops implying the mesoporous structure of the catalysts. The calculation of the surface area is done using the BET method and pore size distribution is done using the BJH method. It has been found that the maximum surface area is found for the ZrPr(4) catalyst with 39 m^2/gm and its pore volume is 0.03 cm^3/gm. With the Pr concentration increase in the catalysts, there is an increase in the surface area and the pore volume that indicates the uniform spreading of Pr in the catalysts, making it more mesoporous. However, as the Pr content increased to 0.05, the surface area decreased due to the absurd sintering of Pr ions and nonporous spreading in the catalyst. It can be stated that the surface area aligns well with the high DMC yield.

The basic properties or the basicity were calculated using CO_2-TPD (Figure S1b) for the catalysts. At a different range of temperatures, TCD signals are analyzed. The peaks here are divided between low, moderate basic, strong basic, and superstrong basic sites. This is done by studying the behavior of the peaks within different temperature ranges (for e.g., the peaks may lie within certain regions at around 200−300 °C).[27−29] To make it more precise, in the domain of 200 °C, there lies the region of the moderate basic sites, and for the stronger basic sites, the temperature ranges from 400 and 600 °C and the super basic sites lie beyond 600 °C. Superstrong basic sites in ZrPr(4) were created as a result of the addition of

https://doi.org/10.1021/acs.iecr.3c00168
Ind. Eng. Chem. Res. 2023, 62, 6920−6931

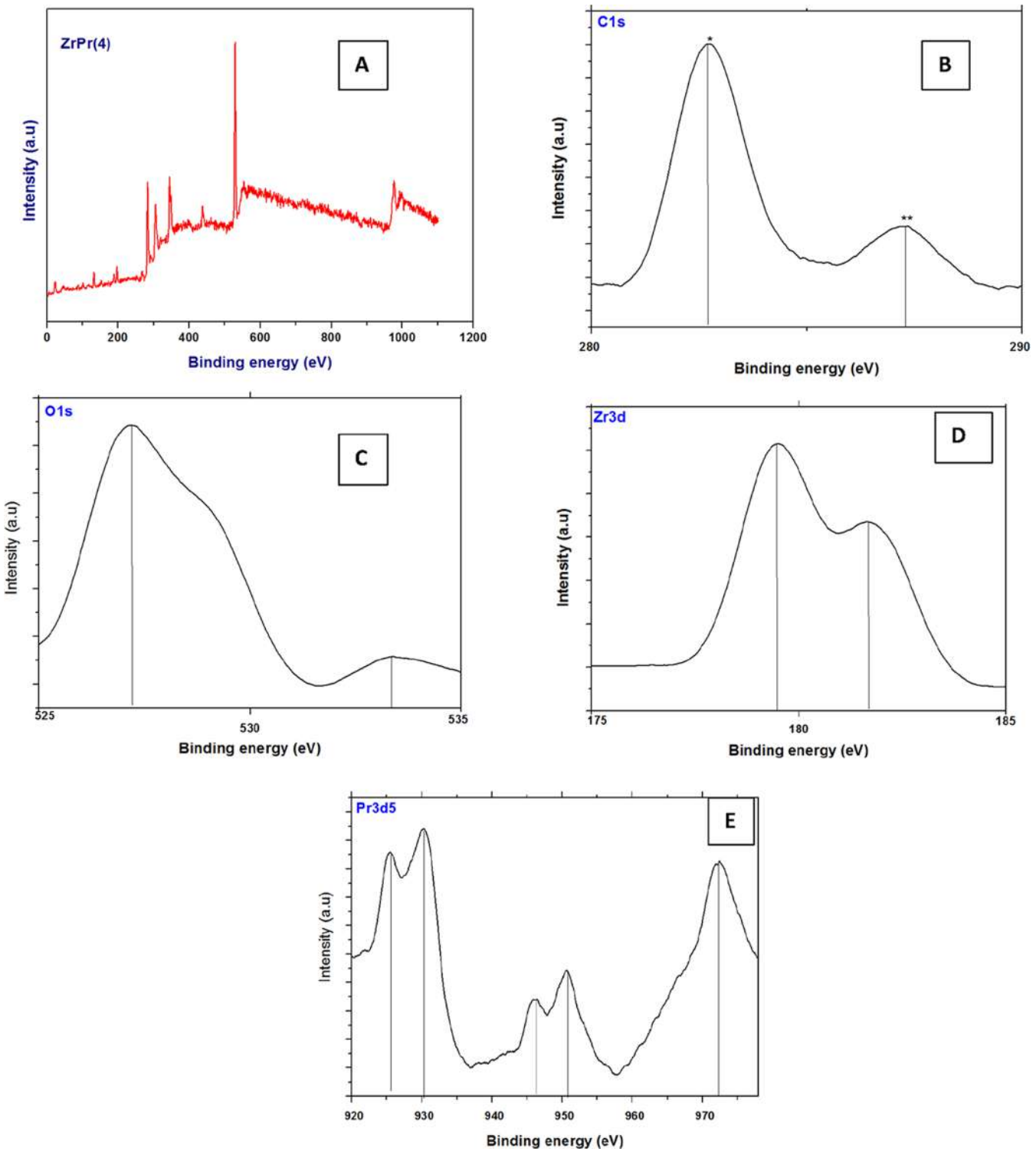

Figure 3. (A) XPS of ZrPr(4), (B) XPS of orbital C_{1s} of ZrPr(4), (C) XPS of orbital O 1s of ZrPr(4), (D) XPS of orbital Zr_{3d} of ZrPr(4), and (E) XPS of orbital Pr_{3d5} of ZrPr(4).

Pr to the catalyst. For the catalyst ZrPr(4), the major peaks are found near 311.5 and 832.1 °C. The calculated basicity for ZrPr(4) is 0.0128 mmol/g. The calculated basicities for ZrPr(1), ZrPr(2), ZrPr(3) and ZrPr(5) are 0.0076, 0.0084, 0.0095, and 0.0099 mmol/g.

XPS of ZrPr(4) determines several functional groups in the catalysts along with the study of the appropriate orbitals present with respect to the binding energy (Figure 3a). The binding energy corresponding to C_{1s}, O_{1s}, Zr_{3d}, and Pr_{3d5} has been shown in Figure 3b−e. There are two visible peaks for C 1s, one around 282.7 eV and the other at 286.9 eV, which relates to C═N and C−O−C (ether/epoxy) according to the deconvoluted spectra.[18] The lattice oxygen and surface oxygen present in the catalyst are demonstrated by peaks in the area between 527 eV and 533.59 eV that are visible in the deconvoluted spectra of O 1s.[9] The fact that there is no

https://doi.org/10.1021/acs.iecr.3c00168
Ind. Eng. Chem. Res. 2023, 62, 6920−6931

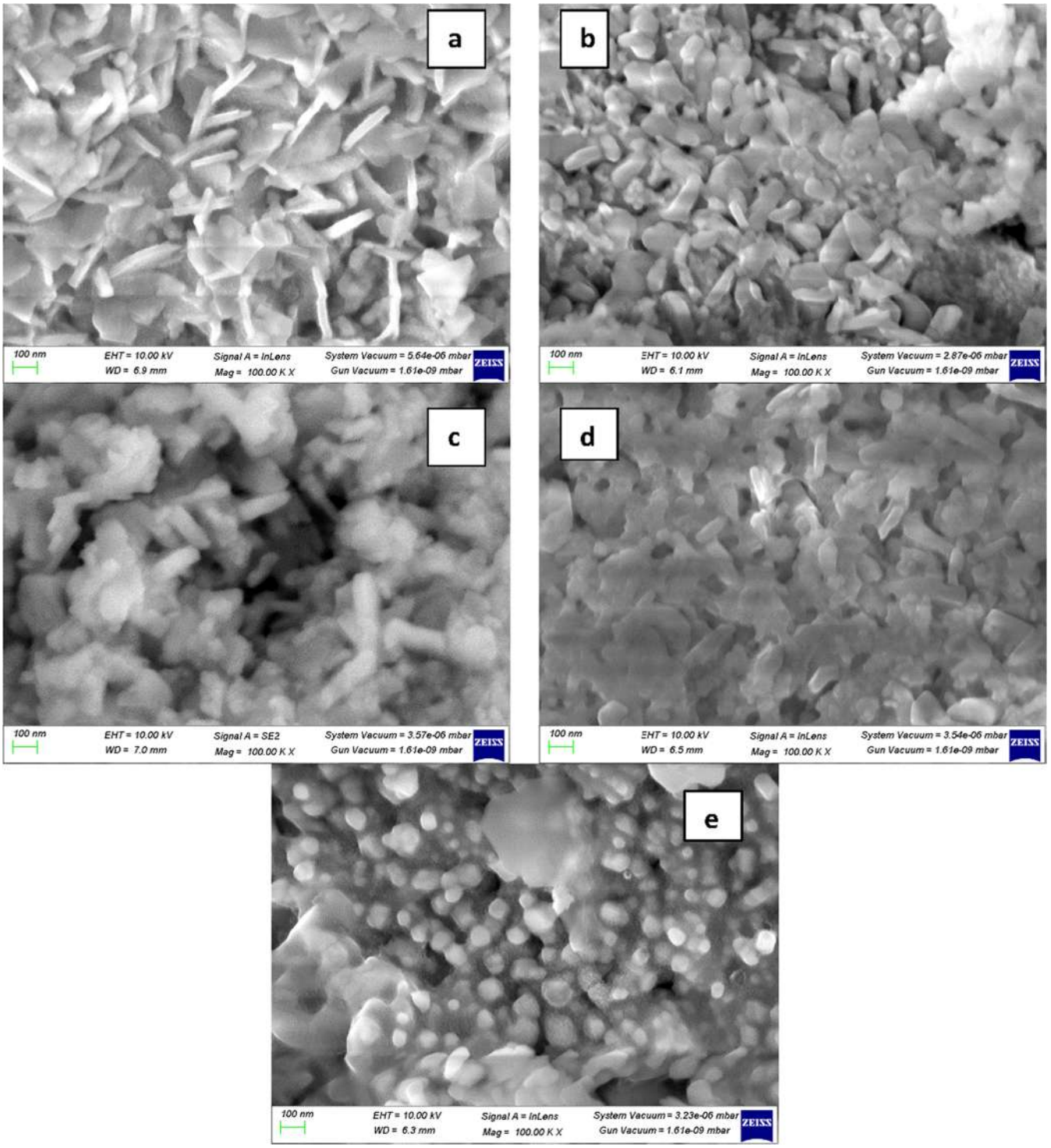

Figure 4. FESEM of (a) ZrPr(1), (b) ZrPr(2), (c) ZrPr(3), (d) ZrPr(4), and (e) ZrPr(5).

distinct O 1s peak that corresponds to ZrO_2 and PrO_2 is further investigated, pointing to the catalyst's status as a homogeneous solid solution with chemical interactions.[9] Similarly, the deconvoluted spectra of O 1s show the peaks in the region at around 527.9 and 533.59 eV that show the presence of lattice oxygen and surface oxygen present in the catalyst.[25] It is also studied that there do not occur any separate O 1s peaks corresponding to ZrO_2 and PrO_2, suggesting that the catalyst is a homogeneous solid solution with chemical interactions.[9] The O 1s peak, which is present near 533.2 eV, reflects the shift toward the lower binding energy, which phenomenally, happens in substituted metal oxides. Such bonds may correspond to the formation of Zr−O−Pr bonds on the external surface of the materials.

The peaks at around 179.4 and 181.7 eV corresponding to Zr_{3d} orbitals state that they are related to the states of $Zr3d_{5/2}$ (suboxides) and $Zr3d_{3/2}$ (suboxides) orbitals, respectively, due to the mixing of Pr in the catalysts, which enables the subreduction of oxides of Zr. Zr_{3d} splits into doublets corresponding to the peaks at 179.4 and 181.7 eV stating the

https://doi.org/10.1021/acs.iecr.3c00168
Ind. Eng. Chem. Res. 2023, 62, 6920−6931

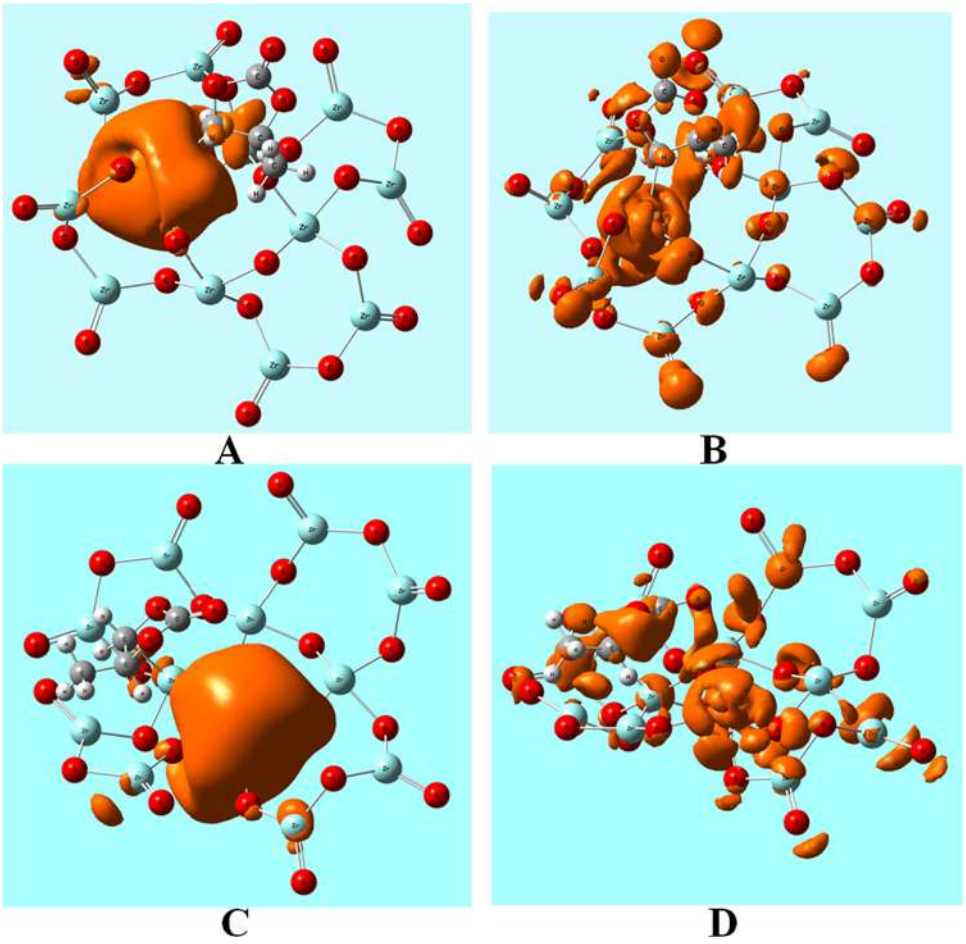

Figure 5. HOMO (A) and LUMO (B) structures of the electronic density of PC adsorbed on the Pr atom of ZrO_2−PrO_2 support. HOMO (C) and LUMO (D) structures of the electronic density of PC adsorbed on the Zr atom of ZrO_2−PrO_2 support.

presence of Zr^{4+} species. The four peaks corresponding to Pr_{3d5} orbitals are found at 925.3, 930.3, 949.5, and 974.6 eV. The peak at around 930.3 eV is related to Pr 3_{d5},[29] whereas it is also found from the XPS data that Pr^{3+} and Pr^{4+} states exist in the catalyst as the peak appears near 930.3 and 949.5 eV, respectively.[21]

The XPS spectra of ZrPr(4) can be studied in Figure 3, through which various states of Pr (Pr^{3+} or Pr^{4+}) may be identified. As already indicated, the Pr^{3+} state is associated with the peak near 930.3 eV, proving that an oxygen vacancy has been created in the lattice. Another peak which is present near 949.5 eV is symbolic of the Pr^{4+} state. These bands will help in quantitatively calculating the concentration of Pr^{3+} states through the equation

$$C[Pr_{3+}] = \left(\frac{A_{Pr3+}}{A_{Pr3+} + A_{Pr4+}}\right)100$$

On calculation, it has been found that the percentage of Pr^{3+} to the total Pr_{total} is 34.9% for ZrPr(4).

Additionally, an oxygen vacancy is a crucial variable for improving the DMC yield during the transesterification of PC and methanol. Accordingly, as the percentage of Pr in the lattice increases, there is a greater chance that Pr^{3+} ions will be present, which will improve the oxygen vacancy. Two distinct peak kinds are mostly identified by the catalysts' O 1s spectra. One is visible near 527.98 eV, whereas the other is visible near 533.2 eV. The peak at 527.9 eV indicates the presence of the lattice oxygen O_L, and the peak at 533.2 eV indicates the presence of O^{2-} (Ov) ions in surface oxygen vacancies. The concentration of surface oxygen vacancies gets calculated via the following formula

$$C[O_v] = \left(\frac{A_{Ov}}{A_{Ov} + A_{OL}}\right)100$$

Through the calculation, it has been found that the concentration of oxygen vacancies ZrPr(4) is 87.27%. For the catalysts, this oxygen vacancy comes out to be 77, 81, 83, and 80% for ZrPr(1), ZrPr(2), ZrPr(3), and ZrPr(5), respectively.

FESEM (Figure 4) enables the morphological study of the catalyst. During the FESEM analysis, it was found that the formation of grains occurred in the catalysts with the mixing of Pr in Zr. The prevalent morphology for ZrPr(1), ZrPr(2), ZrPr(3), and ZrPr(4) retained this type of grain structure. As a result of the improved fixing of Pr^{3+} in Zr ions, this grain type of structure comprises particles with sizes ranging from 1 to 100 nm. Such particle size is consistent when compared to the size determined by the XRD Debye−Scherrer equation. In the case of ZrPr(5), the interaction of Pr with the metallic oxides caused the creation of praseodymium conglomerates in the zirconium, which can be seen in the micrographs. This formation of large particles determines that Pr^{3+} does not fit well in the lattice.[25]

https://doi.org/10.1021/acs.iecr.3c00168
Ind. Eng. Chem. Res. 2023, 62, 6920−6931

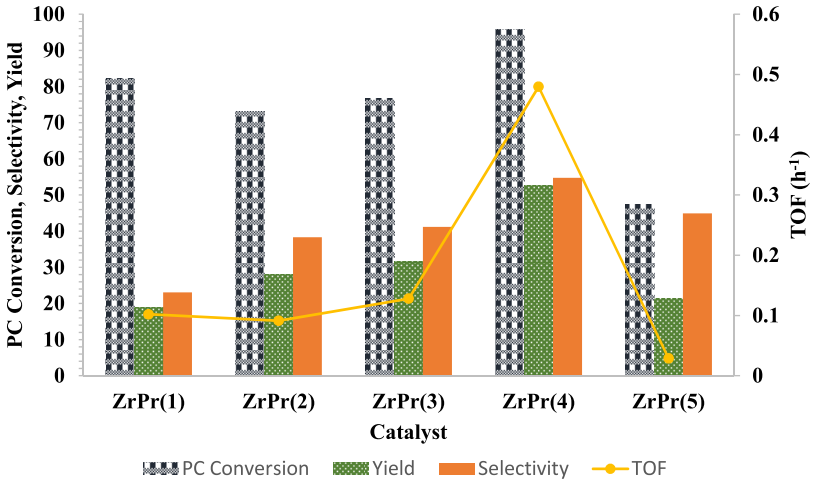

Figure 6. PC conversion, DMC yield, and selectivity at optimum conditions of temperature = 165 °C, methanol/PC ratio = 6.5, catalyst dose = 5 wt % PC, stirring speed = 600−650 rpm, and time = 3 h.

3.2. DFT Calculations. The DFT calculations of the catalytic system were conducted using Gaussian 16W and Gauss View 6.0 software. The optimization of the geometries was carried out using Becke's hybrid three-parameter nonlocal exchange functional (B3) in combination with the Lee−Yang−Parr (LYP) correlation functional (B3LYP) and the SDD basis set.[30−33] All of the calculations are performed considering symmetry.

3.2.1. Geometry. ZrO_2−PrO_2 with a Pr/Zr ratio of 1/11 was employed to study the reaction of PC and methanol via DFT calculations. The two-dimensional structure of the ZrO_2−PrO_2 support is shown in Figure S2a. The average bond lengths of Zr−O and Pr−O in the inner support side are 2.198 and 2.314 Å, respectively.[33] The Zr−O bonds at the periphery of the support have shorter bond lengths with an average value of 1.900 Å. Figure S2b shows the bond lengths of all of the atoms bonding in the ZrO_2−PrO_2 catalyst. ZrO_2 has an average Zr−O bond length of 2.000 and a cage-like shape. The addition of Pr increases the link while preserving the cage-like structure.[33,34] Propylene carbonate (PC) can adsorb on the Zr or Pr atom of the support. Figures S2c,d shows the adsorption of PC on Zr and Pr atoms of the support with respective bond lengths of 2.211 and 2.418 Å, respectively.

3.2.2. Electronic Structure and Properties. Mulliken charge analysis was performed for the ground state. Zirconium and praseodymium had positive charges, and oxygen atoms had a negative charge, which acts as an electron donor. The terminal oxygen has a smaller negative charge than the bridged oxygen. The charge transfer takes place efficiently with zirconium and oxygen atoms on the internal side of the support. Zr and Pr atoms near terminal oxygen atoms have a larger positive charge. Bonding and electronic structures are effectively understood by the visualization of the electronic density of the HOMO and LUMO states.[34] HOMO and LUMO structures for PC adsorbed on Zr of ZrO_2−PrO_2 support are shown in Figure 5a,b, respectively. The concentration of HOMOs is caused by the 2p orbital of terminal oxygen atoms close to the adsorption site (Zr atom).[33] The 4d orbitals of Zr and the 4f orbitals of Pr are where the LUMOs are concentrated. Understanding the HOMO−LUMO gap is crucial to comprehending chemical reactivity.[27] Chemical stability is higher in systems with a larger energy difference between HOMO and LUMO. Figure 7C shows the HOMO structure of PC adsorbed on the ZrO_2−PrO_2 support, while Figure 5D shows the LUMO structure. Comparing PC adsorbed on Pr to PC adsorbed on a Zr atom, the HOMO−LUMO gap narrows somewhat.

ZrO_2 is a polar molecule with a dipole moment of 7.8D, while the pure ZrO_2 support has a dipole moment of 8.4D.[34,35] The presence of the Pr atom in the ZrO_2 cage resulted in an increase of the dipole moment to 11.04 D due to the extra electron cloud of 4F orbitals. The excess electron bounded by the polar bond is localized on the Pr atom. During the transition state, one molecule of PC and one molecule of methanol are adsorbed on the support. As shown in Figure S3a,b, one methanol remains in the bulk phase and interacts directly with the PC molecule. The PC molecule is adsorbed on an adjacent Zr atom, and a bigger electron cloud of Pr adsorbs one methanol atom during the transition state, as shown in Figure S3a. Similarly, the electron cloud of an adjacent Zr atom adsorbs the methanol molecule when PC is adsorbed on the Pr atom. The action of methanol molecules with one on the adjacent active site and the other in the bulk leads to the dissociation of PC molecules, which, in turn, converts into dimethyl carbonate and propylene glycol.

3.3. Catalyst Activity. DMC and PG are the results of the reaction between methanol and propylene carbonate in the presence of the catalyst ZrPr(4) (Figure 6 and Table 2). According to the mechanistic model, it is discovered that the catalysts' surfaces aid in activating the methanol molecule, which produces CH_3O^- and H^+ ions. When this methoxy ion reacts with PC, an intermediate ion known as 2-methyl-hydroxyethyl methyl carbonate is created (2-HMC). DMC and PG are created when this 2-HMC combines with the methoxy

Table 2. Catalyst Performance at Temperature 165 °C, Methanol/PC Ratio = 6.5, Time = 3 h, and Catalyst Dose = 5 wt % of PC

catalysts	PC conversion (%)	DMC yield (%)	TOF (h^{-1})	selectivity
ZrPr(1)	82.18 ± 2	18.99 ± 3	0.102	23.11 ± 2
ZrPr(2)	73.14 ± 3	28.02 ± 4	0.0914	38.31 ± 3
ZrPr(3)	76.75 ± 5	31.61 ± 2	0.128	41.19 ± 3
ZrPr(4)	95.96 ± 3	52.54 ± 3	0.4798	54.75 ± 4
ZrPr(5)	47.46 ± 2	21.31 ± 3	0.029	44.89 ± 3

https://doi.org/10.1021/acs.iecr.3c00168
Ind. Eng. Chem. Res. 2023, 62, 6920−6931

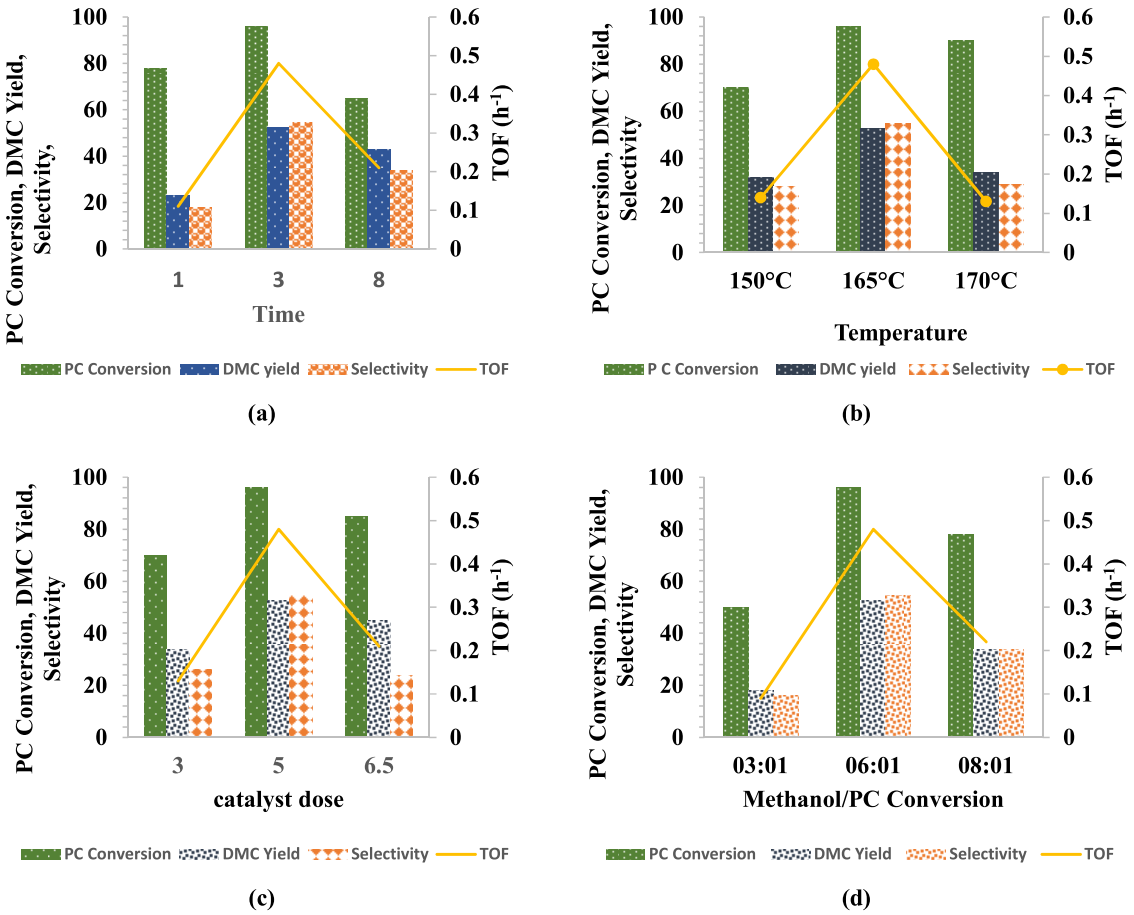

Figure 7. Graphical representation of the effect of operating parameters on PC conversion, DMC yield, selectivity, and TOF using catalyst ZrPr(4). (a) Time (1−8 h), catalyst dose = 5 wt % of PC, temperature = 165 °C, and methanol/PC = 6.5:1; (b) temperature (150−170 °C), time = 3 h, catalyst dose = 5 wt % of PC, and methanol/PC ratio = 6.5:1; (c) catalyst dose (3−6.5 wt % of PC), time = 3 h, methanol/PC ratio = 6.5:1, and temperature = 165 °C; and (d) methanol/PC ratio (3:1−8:1), time = 3 h, temperature = 165 °C, and catalyst dose = 5 wt % of PC.

ion and the hydroxy ion once more. The complete process is investigated over a range of operational parameters, including temperature, time, the ratio of methanol to PC, and the dose of the catalyst. The variance in just one of them impacts DMC production, which, in turn, impacts DMC yield and selectivity.

The catalyst ZrPr(4) is studied in detail with respect to operating parameters like time, temperature, catalyst dose, and methanol/PC ratio. These parameters are varied in a certain ratio and then subjected to the reaction to find out the reaction's optimum conditions.

3.3.1. Time. While other factors such as the catalyst dose, temperature, and methanol/PC ratio are kept constant, the time for the reaction is varied, and it is found out how time affects the reaction yield and selectivity (Figure 7a). Through the study, it is found that the 3 h of the study gave the best yield in terms of PC conversion, DMC yield, and selectivity. When the operating conditions were kept as time = 1 h, catalyst dose = 5 wt % of PC, temperature = 165 °C, and methanol/PC ratio = 6.5, the PC conversion was 78%, DMC yield was 23%, DMC selectivity was 18%, and TOF was found to be 0.11 for the reaction. As the time is increased to 3 h, the PC conversion, DMC yield, and DMC selectivity increase sincerely to 95.96, 52.54, and 54.7%, respectively. The TOF of this reaction is found to be 0.48 h^{-1}. Qin et al.[36] showed that the equilibrium time for the highest yield was 4 h after which there occurs no increase in yield and selectivity. On increasing time to 8 h with other factors remaining constant, the PC conversion, DMC yield, and selectivity declined to 65, 43, and 34%, respectively. This decrease in PC conversion and other factors is due to the formation of an intermediate tending toward the formation of propylene glycol. This is the reason that the formation of DMC is hindered by the increase in time.

3.3.2. Temperature. The study of the effect of temperature is investigated by varying the temperature and keeping other parameters constant (Figure 7b). The temperature is varied between 150 and 170 °C. It is reflected that the maximum PC conversion, DMC yield, and selectivity are achieved at 165 °C being 95.9, 52.5, and 54.7%, respectively. This is the optimum temperature for this reaction. Though this optimum temperature in the presence of nitrogen-functionalized graphene oxide sheets was 180 °C due to the endothermicity of the chemical process,[18] Wang et al.[27] reported 160 °C to be the most optimum condition, where they achieved the maximum yield and selectivity, whereas in this study, when the reaction was carried out at nearly 150 °C, the PC conversion was around 70%, DMC yield and selectivity being 32 and 28%, respectively. A similar reduction was achieved when the temperature was increased to 170 °C, PC conversion was around 90%, whereas the DMC yield and selectivity were lessened to 34 and 29%, respectively. Wei et al.[37] have reported a similar reversal effect on DMC yield and selectivity with higher temperatures. This occurrence happened due to the

https://doi.org/10.1021/acs.iecr.3c00168
Ind. Eng. Chem. Res. 2023, 62, 6920−6931

formation of 2-HMC as an intermediate tending toward the formation of propylene glycol. This high temperature gives the suitability of propylene glycol as the stable temperature for its sustenance.

3.3.3. Catalyst Dose. The catalyst dose is also an important parameter to find out what amount of catalyst should be put in a reaction to get the optimum DMC yield and selectivity (Figure 7c). Initially, when a reactor is put with 3 wt % PC, it gave a PC conversion of 70% and a DMC yield and a selectivity of 34 and 26% were obtained, respectively. This was increased to 95.95% of PC conversion, 52.54% of DMC yield, and 54.74% of DMC selectivity when the catalyst dose was increased to 5 wt % PC. This may be due to the exposure of the surface area of the catalyst and the presence of enough basic sites on the surface for the adsorption of methanol and propylene carbonate, which forms the product DMC. Now, any further increase in catalyst dose led to a hindrance in the reaction due to the sintering of raw materials on the catalyst surface. An increasing amount dose induces higher viscosity of the reaction mixture to increase the mass transfer resistance more than the sintering of the raw material on the active site. Hence, the decline in the PC conversion to 85%, and DMC yield and selectivity to 45 and 24%, respectively, happened when the catalyst dose was 6.5 wt % PC.

3.3.4. Methanol/PC Ratio. The methanol/PC ratio is studied as an important parameter to determine its effect on the reaction of PC with methanol (Figure 7d). It is being found that at a lower methanol/PC ratio, precisely 3:1, DMC yield is low and there is also low PC conversion. The PC conversion was found to be 50.0% and the DMC yield and selectivity of 18 and 16%, respectively. Now when this ratio gets increased to 6:1, it is found that PC conversion reached 95.9%, DMC yield of 52.5%, and DMC selectivity of 54.7%. With the further increase of the methanol/PC ratio to 8:1, the formation of propylene glycol was favored. Here, DMC yield and selectivity decreased to 34 and 29%, respectively. Murugan et al.[38] showed that there was an increase in DMC yield and selectivity until the ratio was 10:1, which decreased after a further increase in the ratio due to the formation of methanol−DMC azeotrope.

3.4. Reusability of the Catalyst. Recycle studies of the catalyst ZrPr(4) have been done by centrifuging the catalyst after the reaction has occurred each time. This catalyst is dried in an oven to eliminate the adsorbed species so that it can be used in the reaction. There is a weight loss in the catalyst after each cycle as there is a loss of the catalyst during the washing process. It has been found that when the catalyst was used for the 1st time, the PC conversion achieved was 95.96% and the DMC yield obtained was 52.54%. When it was used for the 2nd time, the PC conversion reached 77% and the DMC yield was 33%. In the 3rd run of recyclability, 70% PC got converted and the DMC yield obtained was 31%. This result stagnated for further cycles to PC conversion near 65% and DMC yield to 30%. Both the DMC yield and PC conversion declined due to the sintering of the sites that hindered the reaction from occurring on the surface. After five cycles, it became difficult to regenerate the catalyst for further use.

3.5. Future Outlook. The study made for this reaction using zirconium and praseodymium shall have a positive impact in the coming future for the larger scientific community. Various reactions apart from transesterification reactions have shown great impact by using Pr as an important element in the preparation of several catalysts. Ziarani et al.[39] have produced an SBA−Pr−SO_3H catalyst and have shown that this catalyst can be used in several organic reactions. These reactions include an esterification reaction, an etherification reaction, a dehydration reaction, an oxidation reaction, acetylation and acetoxylation reactions, a silylation reaction, and other organic transformations. Using Pr in the catalyst has improved various properties of the catalyst such as better adsorption through lanthanide linkage, basicity, etc., and improved the performance of the reactions in terms of yield and selectivity. Lin and Rajanbabu[40] have shown the role played by $Y_5(O^iPr)_{13}O$ and $thd_2Y(O^iPr)$ as transesterification catalysts. Stoian et al.[20] have shown that doping CeO_2 with several rare-earth metals helps in improving the stability of the catalyst and enhancing the yield of dimethyl carbonate produced through the direct synthesis route. While CeO_2 was doped with several rare-earth metals, Pr as a dopant has the best performance. Hence, Pr as a dopant or even as the main component in the catalyst can play a vital role in carrying out several reactions that include chemical importance.

In making a comparison of several studies done in the field of production of dimethyl carbonate through the transesterification route, it can be shown that using a meager amount of Pr and without altering the intact structure of the catalyst, the performance of the reaction can be improved in terms of yield and selectivity. Xue et al.[41] have used Ce doped on $La_2O_2CO_3$ as a catalyst and have achieved a PC conversion of 85%. Dahiya et al.[42] reported a PC conversion of 81.7% with a DMC selectivity of 71.6% using a $Ti_{0.96}Pr_{0.04}$ catalyst at a temperature of 170 °C. Various catalysts have shown performance better than this work also, like the maximum DMC selectivity obtained was 96.3% with catalyst Ce−Mg−Al by Liao et al.[17] The use of Pr in this work has brought an insight that it can be further mixed with other metal oxides and also be used as a dopant for the better yield and selectivity of DMC.

4. CONCLUSIONS

Through this paper, a study has been conducted in a batch reactor in order to understand the reactivity of methanol with propylene carbonate via a transesterification reaction and the ability of the reaction to produce DMC and propylene glycol. The utilization of a catalyst formed from mixing Zr with Pr was not yet studied for this reaction as per our knowledge. In this work, five sets of catalysts were synthesized by mixing them in different ratios of Zr and Pr named as ZrPr(1), ZrPr(2), ZrPr(3), ZrPr(4), and ZrPr(5). It has been discovered that the use of this catalyst in this reaction results in high PC conversion for ZrPr(4) as well as improved DMC yield and selectivity. The yield and selectivity were 52.5% and 54.7%, respectively, at a temperature of 165 °C, a methanol/PC ratio = 6.5, and a time of 3 h, which were likewise the most ideal operating conditions. It was discovered that the best PC conversion (95.9%) was achieved for ZrPr(4). The presence of basic sites, surface area, and oxygen vacancies was discovered to be the driving factors for this reaction's greater PC conversion. Through calculations, it was discovered that ZrPr(4) has a higher percentage of oxygen vacancies than the other catalysts at 87.3%. DFT calculations showed that Zr and Pr atoms have vast electron clouds, which increases the dipole moment largely with values of 8.4 and 11.04 D in the pure ZrO_2 support and PrO_2−ZrO_2 catalyst, respectively. The PC atoms adsorbed on the Pr atom have a higher tendency to form a product due to the lower HOMO−LUMO gap. Both

https://doi.org/10.1021/acs.iecr.3c00168
Ind. Eng. Chem. Res. 2023, 62, 6920−6931

the investigation and the occurrence of the transesterification of propylene carbonate and methanol aided in the understanding of the process by which methanol is adsorbed on the catalyst surface.

■ ASSOCIATED CONTENT

Supporting Information

The Supporting Information is available free of charge at https://pubs.acs.org/doi/10.1021/acs.iecr.3c00168.

N_2 adsorption−desorption and CO_2-TPD of the catalyst ZrPr(4), two-dimensional structure of ZrO_2−PrO_2 support with a Pr/Zr ratio of 1/11, PC and methanol interaction on ZrO_2−PrO_2 support with PC adsorbed on Pr and Zr atoms, and reuse of catalyst ZrPr(4) at an optimum condition (PDF)

■ AUTHOR INFORMATION

Corresponding Author

Vimal Chandra Srivastava − *Department of Chemical Engineering, Indian Institute of Technology Roorkee, Roorkee, Uttarakhand 247667, India;* orcid.org/0000-0001-5321-7981; Phone: +91-1332-285889; Email: vimalcsr@yahoo.co.in, vimal.srivastava@ch.iitr.ac.in; Fax: +91-1332-27635

Authors

Surbhi Dahiya − *Department of Chemical Engineering, Indian Institute of Technology Roorkee, Roorkee, Uttarakhand 247667, India*

Pankaj Kumar − *Department of Chemical Engineering, Indian Institute of Technology Roorkee, Roorkee, Uttarakhand 247667, India;* orcid.org/0000-0003-3686-257X

Vimal Kumar − *Department of Chemical Engineering, Indian Institute of Technology Roorkee, Roorkee, Uttarakhand 247667, India;* orcid.org/0000-0002-2140-7454

Complete contact information is available at: https://pubs.acs.org/10.1021/acs.iecr.3c00168

Notes

The authors declare no competing financial interest.

■ ACKNOWLEDGMENTS

The authors are thankful to the Science and Engineering Research Board, Department of Science and Engineering Research Board, Department of Science & Technology, Government of India, New Delhi, for providing financial help for carrying out this research work under the project (EMR/2016/007510).

■ REFERENCES

(1) Prymak, I.; Prymark, O.; Wang, J.; Kalevaru, V. N.; Martin, A.; Bentrup, U.; Wohlrab, S. Phosphate functionalization of CeO_2-ZrO_2 solid solutions for the catalytic formation of dimethyl carbonate from methanol and carbon dioxide. *ChemCatChem* **2018**, *10*, 391−394.

(2) Pyo, S. H.; Park, J. H.; Chang, T. S.; Hatti-Kaul, R. Dimethyl carbonate as a green chemical. *Curr. Opin. Green Sustainable Chem.* **2017**, *5*, 61−66.

(3) Faria, D. J.; Santos, L. M. D.; Bernard, F. L.; Pinto, I. S.; Resende, M. A. D. M.; Einloft, S. Dehydrating agent effect on the synthesis of dimethyl carbonate directly from methanol and carbon dioxide. *RSC Adv.* **2020**, *10*, 34895.

(4) Zhang, Z.; Liu, S.; Zhang, L.; Yin, S.; Yang, G.; Han, B. Driving dimethyl carbonate synthesis from CO_2 and methanol and production of acetylene simultaneously using CaC_2. *Chem. Commun.* **2018**, *54*, 4410.

(5) Pu, Y.; Xuan, K.; Wang, F.; Li, A.; Zhao, N.; Xiao, F. Synthesis of dimethyl carbonate from CO_2 and methanol over a hydrophobic Ce/SBA-15 catalyst. *RSC Adv.* **2018**, *8*, 27216.

(6) Zhang, M.; Alferov, K. A.; Xiao, M.; Han, D.; Wang, S.; Meng, Y. Continuous dimethyl carbonate synthesis from CO_2 and methanol using Cu-Ni@VSiO as catalyst synthesized by a novel sulfuration method. *Catalysts* **2018**, *8*, 142.

(7) Abdalla, A. O. G.; Liu, D. Dimethyl carbonate as a promising oxygenated fuel for combustion: A Review. *Energies* **2018**, *11*, 1552.

(8) Tamboli, A. H.; Chaugule, A. A.; Kim, H. Catalytic developments in the direct dimethyl carbonate synthesis from carbon dioxide and methanol. *Chem. Eng. J.* **2017**, *323*, 530−544.

(9) Fu, Z.; Zhong, Yu. Y.; Long, L.; Xiao, M.; Han, D.; Wang, S.; Meng, Y. TiO_2 Doped CeO_2 Nanorod Catalysts for Direct Conversion of CO_2 and CH_3OH to Dimethyl Carbonate: Catalytic Performance and Kinetic Study. *ACS Omega* **2018**, *3*, 198−2017.

(10) Chen, Y.; Wang, H.; Qin, Z.; Tian, S.; Ye, Z.; Ye, L.; Abroshan, H.; Gao, L. $Ti_xCe_{1-x}O2$ nanocomposites: A monolithic catalyst for direct conversion of carbon dioxide and methanol to dimethyl carbonate. *Green Chem.* **2019**, *21*, 4642.

(11) Marin, C. M.; Li, L.; Bhalkikar, A.; Doyle, J. E.; Zheng, X. C.; Cheung, C. L. Kinetic and mechanistic investigations of the direct synthesis of dimethyl carbonate from carbon dioxide over ceria nanorod catalysts. *J. Catal.* **2016**, *340*, 295−301.

(12) Nivangune, N.; Kelkar, A. Selective synthesis of dimethyl carbonate via transesterification of propylene carbonate with methanol catalyzed by bifunctional Li-Al nano-composite. *ChemistrySelect* **2019**, *4*, 8574−8583.

(13) Song, Z.; Jin, X.; Hu, Y.; Subramaniam, B.; Chaudhari, R. V. Intriguing Catalyst (CaO) Pretreatment Effects and Mechanistic Insights during Propylene Carbonate Transesterification with Methanol. *ACS Sustainable Chem. Eng.* **2017**, *5*, 4718−4729.

(14) Wang, H.; Wang, M.; Zhang, W.; Zhao, N.; Wei, W.; Sun, Y. Synthesis of dimethyl carbonate from propylene carbonate and methanol using CaO-ZrO_2 solid solutions as highly stable catalysts. *Catal. Today* **2006**, *115*, 107−110.

(15) Pyrlik, A.; Hoelderich, W. F.; Muller, K.; Arlt, W.; Strautmann, J.; Kruse, D. Dimethyl carbonate via transesterification of propylene carbonate with methanol over ion exchange resins. *Appl. Catal., B* **2012**, *125*, 486−491.

(16) Kumar, P.; Srivastava, V. C.; Mishra, I. M. Dimethyl carbonate synthesis via transesterification of propylene carbonate with methanol by ceria-zinc catalysts: Role of catalyst support and reaction parameters. *Korean J. Chem. Eng.* **2015**, *32*, 1774−1783.

(17) Liao, Y.; Li, F.; Dai, X.; et al. Solid base catalysts derived from Ca-M-Al (M = Mg, La, Ce, Y) layered double hydroxides for dimethyl carbonate synthesis by transesterification of methanol with propylene carbonate. *Chin. J. Catal.* **2017**, *38*, 1860−1869.

(18) Kumar, N.; Srivastava, V. C. Dimethyl carbonate production via transesterification reaction using nitrogen functionalized graphene oxide nanosheets. *Renewable Energy* **2021**, *175*, 1−13.

(19) Su, W.; Chen, J.; Wu, L.; Wang, X.; Wang, X.; Fu, X. Visible light photocatalysts on praseodymium(III)-nitrate modified TiO_2 prepared by an ultrasound method. *Appl. Catal., B* **2008**, *77*, 264−271.

(20) Stoian, D.; Medina, F.; Urakawa, A. Improving the stability of CeO_2 catalyst by rare earth metal promotion and molecular insights in the Dimethyl Carbonate Synthesis from CO_2 with 2-Cyano-pyridine. *ACS Catal.* **2018**, *8*, 3181−3193.

(21) Zhang, Z.; Wang, Y.; Lu, J.; Zhang, J.; Li, M.; Liu, X.; Wang, F. Pr-doped CeO_2 catalyst in prins condensation-hydrolysis reaction: Are all defect sites catalytically active. *ACS Catal.* **2018**, *8*, 2635−2644.

(22) de Rivas, B.; Hurtado, N. G.; Fonseca, R. P.; Pascual, F. C.; Garcia, A. G.; Ortiz, J. I. G.; Lopez, A. B. Activity, selectivity and stability of praseodymium-doped CeO_2 for chlorinated VOCs catalytic combustion. *Appl. Catal., B* **2012**, *121−122*, 162−170.

(23) Kumar, N.; Srivastava, V. C. Dimethyl Carbonate Synthesis via Transesterification of Propylene Carbonate Using an Efficient Reduced Graphene Oxide- Supported ZnO Nano catalyst. *Energy Fuel* **2020**, *34*, 7455−7464.
(24) Song, Z.; Subramaniam, B.; Chaudhari, R. V. Intriguing catalyst (CaO) pretreatment effects and mechanistic insights during propylene carbonate transesterification with methanol. *ACS Sustainable Chem. Eng.* **2019**, *7*, 5698−5710.
(25) Ramos-Brito, F.; Hipolito, M. G.; Armenta, C. A.; Fragoso, O. A.; Falcony, C. Characterization of luminescent praseodymium-doped ZrO_2 coatings deposited by ultrasonic spray pyrolysis technique. *J. Phys. D: Appl. Phys.* **2007**, *40*, 6718−6724.
(26) Liu, B.; Li, C.; Zhang, G.; Yao, X.; Chuang, S. S. C.; Li, Z. Oxygen vacancy promoting dimethyl carbonate synthesis from CO_2 and methanol over Zr-doped CeO_2 nanorods. *ACS Catal.* **2018**, *8*, 10446−10456.
(27) Wang, H.; Wang, M.; Liu, S.; Zhao, N.; Wei, W.; Sun, Y. Influence of preparation methods on the structure and performance of CaO-ZrO_2 catalyst for the synthesis of dimethyl carbonate via transesterification. *J. Mol. Catal. A: Chem.* **2006**, *258*, 308−312.
(28) Kumar, P.; Srivastava, V. C.; Mishra, I. M. Synthesis of dimethyl carbonate by transesterification reaction using ceria-zinc oxide catalysts prepared with different chelating agents. *Appl. Clay Sci.* **2017**, *150*, 275−281.
(29) Kumar, P.; Srivastava, V. C.; Mishra, I. M. Dimethyl carbonate synthesis by transesterification of propylene carbonate with methanol: Comparative assessment of Ce-M (M=Co, Fe, Cu and Zn) catalysts. *Renew. Energ.* **2017**, *88*, 457−464.
(30) Qiu, G.; Wang, M.; Wang, G.; Diao, X.; Zhao, D.; Du, Z.; Li, Y. Structure and electronic properties of Pd clusters and their interactions with single S atom studied by density-functional theory. *J. Mol. Struct.: THEOCHEM.* **2008**, *861*, 131−136.
(31) Liu, B.; Li, C.; Zhang, G.; Yan, L.; Li, Z. Direct synthesis of dimethyl carbonate from CO_2 and methanol over CaO-CeO_2 catalysts: the role of acid-base properties and surface oxygen vacancies. *New J. Chem.* **2017**, *41*, 12231−12240.
(32) Chiang, C. L.; Lin, K. S.; Yu, S. H. Preparation and characterization of $H_3PW_{12}O_{40}/ZrO_2$ catalyst for carbonation of methanol into dimethyl carbonate. *Res. Chem. Intermed.* **2018**, *44*, 3797−3811.
(33) Zhao, Y.; Truhlar, D. G. A new local density functional for main-group thermochemistry, transition metal bonding, thermochemical kinetics, and noncovalent interactions. *J. Chem. Phys.* **2006**, *125*, No. 194101.
(34) Zhao, Y.; Truhlar, D. G. The M06 suite of density functionals for main group thermochemistry, thermochemical kinetics, noncovalent interactions, excited states, and transition elements: two new functionals and systematic testing of four M06-class functionals and 12 other functionals. *Theoretical Chem. Acc.* **2008**, *120*, 215−241.
(35) Jin, R.; Zhang, Y.; Huang, S.; Wang, P.; Tian, P. Stability, Infrared Spectra and Electronic Structures of (ZrO_2) n (n = 3−6) Clusters: DFT Study. *Chin. J. Chem.* **2011**, *29*, 13−20.
(36) Wang, Q.; Li, F.; Zhao, H.-h.; Kuang, Z.-q.; Wang, F.; LI, L.; Zhao, N.; Xiao, F.-k. Preparation of Mg-Al based solid base for the transesterification of propylene carbonate and methanol. *J. Fuel Chem. Technol.* **2020**, *48*, 448−455.
(37) Wei, T.; Wang, M.; Wei, Z. T.; Sun, Y.; Zhong, B. Effect of base strength and basicity on catalytic behavior of solid bases for synthesis of dimethyl carbonate from propylene carbonate and methanol. *Fuel Process. Technol.* **2003**, *83*, 175−182.
(38) Murugan, C.; Bajaj, H. C. Transesterification of propylene carbonate and methanol using Mg-Al-CO_3 hydrotalcite as solid base catalyst. *Ind. J. Chem.* **2010**, *49A*, 1182−1188.
(39) Ziarani, G. M.; Lashgari, N.; Badiei, A. Sulfonic-acid functionalized mesoporous silica (SBA-Pr-SO_3H) as solid acid catalyst in organic reactions. *J. Mol. Catal. A: Chem.* **2015**, *397*, 166−191.
(40) Lin, M.-H.; Rajanbabu, T. V. Metal−catalyzed acyl transfer reactions on enol esters: Role of $Y_5(O^iPr)_{13}O$ and $thd_2Y(O^iPr)$ as transesterification catalysts. *Org. Lett.* **2000**, *2*, 997−1000.
(41) Xue, Y.; Yu, Z.; Zhai, S.; Li, C.; Wei, X.; Xu, J.; Wang, F.; Xue, B. The role of Ce doping on the activity of $La_2O_2CO_3$ nanosheets catalysts in synthesis of dimethyl carbonate from propylene carbonate and methanol. *Catal. Commun.* **2022**, *171*, No. 106526.
(42) Dahiya, S.; Srivastava, V. C.; Kumar, V. Dimethyl carbonate synthesis via transesterification of propylene carbonate using a titanium−praseodymium-based catalyst. *Energy Fuels* **2022**, *36*, 13148−13158.

https://doi.org/10.1021/acs.iecr.3c00168
Ind. Eng. Chem. Res. 2023, 62, 6920−6931